Registration Using Segment Intensity Remapping and Mutual Information

Zeger F. Knops[1], J.B.A. Maintz[1], M.A. Viergever[1,2], and J.P.W. Pluim[2]

[1] Utrecht University, Department of Computer Science, PO Box 80089, NL-3508TB Utrecht, The Netherlands. {zeger,twan}@cs.uu.nl.
[2] University Medical Center Utrecht, Image Sciences Institute, PO Box 85500, NL-3508GA Utrecht, The Netherlands. {max,josien}@isi.uu.nl.

Abstract. A method for processing images prior to normalized mutual information based registration and an enhancement of the registration measure are presented. The method relies on k-means clustering of the intensity distribution and a gray-value remapping of spatially unconnected segments of similar intensity. Registration experiments using binary images from the MPEG-7 dataset and retinal images show our preprocessing to cause a significant reduction of the number of misregistrations without loss of accuracy or an increase in optimization steps.

1 Introduction

Image registration is a task required in many image processing applications where two or more similar images are involved. To exploit complementary information or express differences these images are often spatially aligned, i.e., registered.

Image content based registration uses the full intensity contents of the image or of a processed image. A measure of registration is defined and the images are assumed to be brought into registration by optimizing this measure. Well established measures include cross-correlation, mutual information and normalized mutual information.

Normalized mutual information (NMI) has proven to be a robust and accurate image registration measure for both mono- and multi-modality image registration [2,1,9,10,8]. During NMI-based registration an estimation of the image intensity distribution is necessary. The most common way to estimating an intensity distribution is by creating a histogram with equidistant binning. In this manner, the boundaries of the bins to be placed at arbitrary gray values rather than at locations meaningful to image structure. This could degrade the image alignment or registration process with respect to the number of misregistrations and speed [3,4]. In this paper we use an alternative binning method based on k-means clustering in order to compensate [3,4].

In an intensity histogram there is no distinction between multiple structures with similar intensities. They all fall into the same bin. This can negatively affect the registration process. We present a new technique, segment remapping,

C. Barillot, D.R. Haynor, and P. Hellier (Eds.): MICCAI 2004, LNCS 3216, pp. 805–812, 2004.

in order to compensate for this effect: segments that are spatially unconnected but have equal intensity are each remapped to a new distinct intensity, e.g., in our "o" example the inside will be mapped to a new distinct intensity.

In section 2 we introduce our approach of combining NMI-based registration with both k-means clustering and segment remapping. We present the materials in section 3. In section 4 we discuss the results of registration with our new approach. Our conclusions are presented in section 5.

2 Methods

2.1 Normalized Mutual Information

The Shannon entropy H for image A with intensities a, n voxels and d distinct intensities is defined as

$$H(A) = -\sum_{a} p_A(a) \log p_A(a) = \log n - \frac{\sum_{x=1}^{d} f(a_x) \log f(a_x)}{n}, \tag{1}$$

where $f(a)$ is the number of voxels with intensity a and $p_A(a)$ is the probability of intensity a in image A.

The Shannon entropy of of two images A and B is defined as

$$H(A, B) = -\sum_{a,b} p_{AB}(a, b) \log p_{AB}(a, b), \tag{2}$$

where $p_{AB}(a, b)$ is the probability of intensity couple (a, b) of corresponding points in the overlapping part of A and B. A joint-histogam is generally used to compute the Shannon entropy for overlapping images. Note that increasing joint-histogram dispersion indicates a reduction in the registration quality.

A registration measure attuned to this effect is normalized mutual information, which is a well established registration measure [7,8,3,4] based on the Shannon entropy of the images:

$$\mathrm{NMI}(A, B) = \frac{H(A) + H(B)}{H(A, B)}. \tag{3}$$

2.2 Intensity Distribution Estimation

In order to compute the NMI of the overlapping part of two images their intensity distribution has to be estimated. Generally this is done by using a histogram with a fixed number of bins and a fixed number of gray values pooled in each bin. Gray values are converted to bin numbers in a rounded linear fashion. Remapping image intensities to bin numbers as described above could split segments over multiple bins, hence influencing the registration process with respect to the number of misregistrations and speed [3,4]. In this paper, we use k-means clustering based binning which takes the intensity distribution itself into account in

order to reduce the splitting of segments. In previous work [3,4] we already have shown that adding k-means clustering based binning to NMI-based registration of 3D medical images (CT/MRI/SPECT) may greatly reduce the number of misregistrations and computational time of the process.

2.3 Segment Remapping

With equidistant binning spatially unconnected structures of similar gray value may be mapped to the same bin. This effect potentially degrades the registration process.

For example, consider an image where both the background and a large segment P have intensity a, and a corresponding image where the large segment P corresponds to a segment Q with intensity b. NMI uses the joint-histogram to determine the quality of the registration. As the overlap of segments P and Q increases so does the histogram entry (a, b) which indicates an increase of registration quality. On the other hand, overlapping segment Q with background, which clearly is not a good registration, also results in an increase of intensity couples (a, b) but not in an increase of registration quality.

We can compensate for this by remapping the intensities of spatially unconnected segments with equal intensity to distinct intensities. In our previous example we would, e.g., remap the intensity of the large segment P to c thus enabling NMI to distinguish between overlap of background and segment Q and overlap of segment P and Q.

2.4 Combining k-Means Clustering and Segment Remapping

A combination of both the standard NMI method and k-means clustering with segment remapping could enhance the registration with respect to the number of misregistrations and speed. We start by remapping the image intensities according to the pre-computed remapping function $k(i)$ where i is the intensity of voxel v. This function is based on the k-means clustering of the original intensity distribution of the image. See [3] and [4] for details of the computation of $k(i)$.

Next, a segment remapping of the image is done. First by determining the number of spatially unconnected segments and their respective size (using a 4-neighbor connectedness filter) for each bin. Second, by assigning a new distinct intensity to each segment. Note that the remapping function depends on the spatial location of the voxel v. Remapping starts with the largest segment. Remapping is stopped when a predetermined percentage of the image has been remapped. This avoids the creation of large numbers of spurious small segments for example, single voxel noise. We define the remapping function for voxel v as $r_v(i)$. Note that for a certain portion of the image the intensity is not affected by the segment remapping procedure.

2.5 Incorporating k-Means Clustering and Segment Remapping into the Standard NMI Framework

We include both the binned and the k-means clustered segment remapped image in the registration measure. We already noted that the regular binning method performs quite well in many circumstances, yet combining our method, $r_v(i)$, and the regular method could further enhance the registration process.

We first define the binning function $b(i)$. Next, we assign a vector s to each image voxel with intensity i according to:

$$s = (b, r) = (b(i), r_v(k(i))), \tag{4}$$

where b is intensity i after applying the binning procedure.

Using the standard NMI approach an overlap of images A and B results in a joint-histogram with intensity couples (b_A, b_B). Our approach results in four distinct intensity couples for each corresponding voxel pair: (b_A, b_B), (b_A, r_B), (r_A, b_B) and (r_A, r_B), forming four distinct joint-histograms. For each of the images we define the entropy of the remapped intensities as $H(A_r)$ for image A and $H(B_r)$ for image B. We define four NMI equations based on (3):

$$NMI_{bb}(A, B) = \frac{H(A_b) + H(B_b)}{H(A_b, B_b)}, \tag{5}$$

$$NMI_{br}(A, B) = \frac{H(A_b) + H(B_r)}{H(A_b, B_r)}, \tag{6}$$

$$NMI_{rb}(A, B) = \frac{H(A_r) + H(B_b)}{H(A_r, B_b)}, \tag{7}$$

$$NMI_{rr}(A, B) = \frac{H(A_r) + H(B_r)}{H(A_r, B_r)}, \tag{8}$$

where subscripts b denote use of grey value employing the standard binning method and subscripts r indicate the use of clustered and remapped intensities.

Note that (5) is equal to the original NMI measure. Image registration can be performed using a combination of measures (5), (6), (7) and (8). Since each NMI measure contains image information that may be relevant to the registration process, we use the measure

$$NMI_s(A, B) = NMI_{bb}(A, B) + NMI_{br}(A, B) + NMI_{rb}(A, B) + NMI_{rr}(A, B), \tag{9}$$

in our experiments.

3 Materials

Three 2D datasets have been used in this study, an artificial test image, the MPEG-7 dataset [5] and a medical retina dataset.

The artificial test image is a 1000 pixels square image, see figure 1(a), consisting of four distinct intensities $(1, 2, 3, 4)$ and eight spatially unconnected segments. This image was created so that some of the unconnected segments have equal intensity and are remapped by our method, see figure 1, in order to detect any changes in the parameter space for NMI_s(b) as compared to standard NMI.

The MPEG-7 data consists of a large number of test images, we randomly selected 50 images from the 'Regionn' part of the dataset. The complete 'Regionn' set is comprised of 3.628 images, however many of those images are made by applying a transformation to the same image, those were not used in our experiments. The data consists of binary images of 128 pixels square.

The retina data consists of 30 images of 768 by 527 pixels with a 8 bit pixel depth of the retina of a single healthy patient. The images were made in a single session during which a contrast agent was administered to the patient. The field of view was 40 by 25 degrees.

4 Experiments and Results

NMI_{bb} based registration, i.e., regular NMI-based registration was compared to NMI_s based registration. To optimize both measures as a function of 2D affine geometric transformations Powell's method was used [6]. The number of optimization steps needed to converge were used as a measure of computational speed. All images except the artificial image were registered to themselves by applying an offset transformation as initial starting position for the registration. The experiment using the artificial image is included only to demonstrate the added value of our new method, which is made clear by a parameter space cut.

4.1 Artificial Image

The artificial 2D image A consists of eight spatially unconnected segments but contains four distinct intensities $(1, 2, 3, 4)$. Intensities 2 and 4 both contain three unconnected segments. Applying our method results in a new image containing eight spatially unconnected segments and eight distinct intensities. The image is shown in figure 1.

A parameter space cut was made by registering the image to itself and applying a rotational offset T. Both the $NMI(A, T(A))$ and the $NMI_{rr}(A, T(A))$ were computed at 1440 equally spaced points comprising a full 360° rotation. To reduce the effects of varying overlap area, the background intensity was not used in the computation. The results can be seen in figure 2.

There is no difference between the two methods with respect to local and global maxima. However, there is a clear difference around the global optimum, whose base has a width of about 10 degrees using $NMI(A, A)$ and a width of

about 80 degrees when using $NMI_{rr}(A, A)$. It is likely an optimization routine such as Powell or hill-climbing will use more optimization steps when using $NMI(A, A)$ instead of $NMI_{rr}(A, A)$.

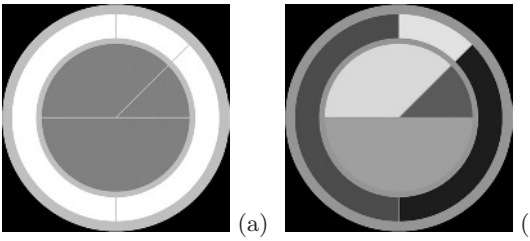
(a) (b)

Fig. 1. The artificial image (1000 pixels square) has four distinct intensities (left) and eight spatially unconnected segments. On the right the same image is shown after remapping has been applied.

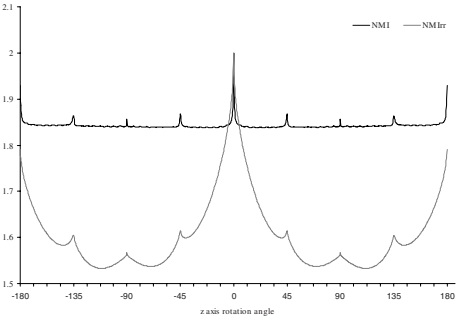

Fig. 2. $NMI(A, T(A))$ and $NMI_{rr}(A, T(A))$ of the artificial image (figure 1a) and a rotated version of the image, for rotation angles form -180 to 180 degrees.

4.2 MPEG-7 Data

Fifty binary were used in the experiment, which were clustered or binned using two bins and 100% binning. Each of the images was registered to itself with an initial null transform which corresponds to correct alignment. A rotation offset of -15, -30, 15 or 30 degrees, a translation offset of -10, -20, 10 or 20 pixels and a scaling of -10, -5, 5 or 10 percent was applied, resulting in 1024 registration starting positions for each image. For each of the registration measures $NMI(A, A)$ and $NMI_s(A, A)$ 51.200 registrations were done. The registration was considered a misregistration if the error was above 0.1 pixel. Some images used in this experiment are shown in figure 3.

Registering the images using both methods resulted in 58% misregistrations for $NMI(A, A)$ and 6% misregistrations for our NMI_s. There were no significant differences for both methods with respect to the number of optimization steps needed for a correct registration.

Fig. 3. Part of the MPEG-7 data used in our experiments.

4.3 Retina Data

Each retina image was registered to itself, using 32 bins for the $NMI(A, A)$ method. For $NMI_s(A, A)$ we used six to eight clusters and 80 to 90 percent segmentation depending on the images. The segmentation percentage was initially set to 80 and then increased until a remapping of large numbers of small segments occurred. Using these parameters resulted in 21 to 83 segments. An example image is shown in figure 4. Each image was registered to itself with an initial null transform which corresponds to correct alignment. A rotation offset of -20, -15, 15 or 20 degrees and a translation offset of -40, -20, 20 or 40 was applied, resulting in 64 starting positions for each image.

Ten images were registered using both methods resulting in 29% misregistrations for the $NMI(A, A)$ method and 9% misregistrations for $NMI_s(A, A)$. Registrations were considered a misregistration if the error was above 0.1 mm. There was no significant difference between the number of optimization steps used for both methods.

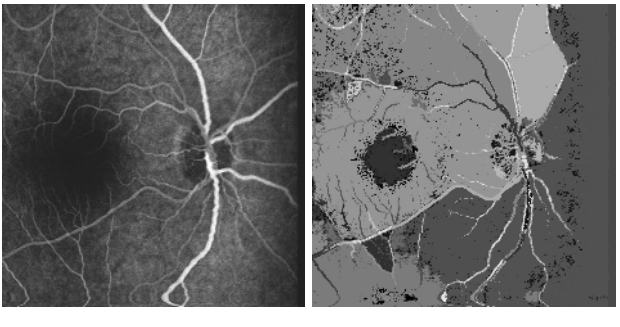

Fig. 4. A retina dataset after binning using 32 bins (left) and after applying our method using 6 clusters and adding 75 segments which comprised 90% of the image (right).

5 Conclusion and Discussion

In summary the combined use of k-means clustering and segment remapping improves the registration process with respect to the number of misregistrations when registering simple binary images or retina images. A parameter space cut made on an artificial image with four distinct intensities and eight spatially unconnected segments with equal intensity shows a significant improvement in the parameter space with respect to the standard NMI measure. Using our method on images with similar properties, i.e. several large spatially unconnected segments with equal intensity, could enhance the parameter space.

A drawback of our method is the presently manual selection of two parameters, the number of clusters and the percentage of the image to be segmented. However, this is a task that can in all likelihood be automated.

Future work will include the suggested automation and the investigation of the practical impact of the $NMI_s(A, A)$ measure on 2D and 3D medical image registration applications.

References

1. A. Collignon. *Multi-modality medical image registration by maximization of mutual information.* PhD thesis, Catholic University of Leuven, 1998.
2. A. Collignon, F. Maes, D. Delaere, D. Vandermeulen, P. Suetens, and G. Marchal. Automated multi-modality image registraction based on information theory. *Information Processing in Medical Imaging*, pages 263–274, 1995.
3. Z.F. Knops, J.B.A. Maintz, M.A. Viergever, and J.P.W. Pluim. Normalized mutual information based registration using K-means clustering based histogram binning. In M. Sonka and J.M. Fitzpatrick, editors, *SPIE Medical Imaging*, volume 5032, pages 1072–1080. SPIE press, 2003.
4. Z.F. Knops, J.B.A. Maintz, M.A. Viergever, and J.P.W. Pluim. Normalized mutual information based PET-MR registration using K-means clustering and shading correction. In J.C. Gee, J.B.A. Maintz, and M.W. Vannier, editors, *International Workshop on Biomedical Image Registration*, volume 2717 of *Lecture Notes in Computer Science*, pages 31–39. Springer, 2003.
5. MPEG-7 "Multimedia Content Description Interface" Documentation. WWW page, http://www.darmstadt.gmd.de/mobile/MPEG7, 1999.
6. W. H. Press, S.A. Teukolsky, W.T. Vetterling, and P.F. Brian. *Numerical recipes in C (2nd ed.): the art of scientific computing.* Cambridge University Press, 1992.
7. C. Studholme. *Measures of 3D medical image alignment.* PhD thesis, University of London, 1997.
8. C. Studholme, D.J. Hawkes, and D.L.G. Hill. An overlap invariant entropy measure of 3d medical image alignment. *Pattern Recognition*, 32(1):71–86, 1999.
9. P. Viola. *Alignment by maximization of mutual information.* PhD thesis, Massachusetts Institute of Technology, 1995.
10. W. M. Wells III, P. Viola, H. Atsumi, S. Nakajima, and R. Kikinis. Multi-modal volume registration by maximization of mutual information. *Medical Image Analysis*, 1(1):35–51, 1996.